Article

Bionic Shape Memory Polyurethane/Prussian Blue Nanoparticle-Based Actuators with Two-Way and Programmable Light-Driven Motions

Xiaofei Wang, Yang He, and Jinsong Leng*

Cite This: ACS Appl. Polym. Mater. 2023, 5, 1398–1408

Read Online

ACCESS | Metrics & More | Article Recommendations | SI Supporting Information

ABSTRACT: A bionic smart actuator that can imitate types of biological motions plays a vital role in intelligent systems, which therefore becomes one of the hottest development directions in recent years and has attracted more and more attention from researchers. In this study, a kind of near-infrared (NIR) light-responsive shape memory polyurethane SMPU-PB is developed by doping the citric acid-modified Prussian blue nanoparticles. Based on it, a bionic "athlete" has performed repeatable photomechanical jumping behavior to cross obstacles under 808 nm NIR light irradiation. Furthermore, through the integration of SMPU-PB with pre-strained UV-responsive polyurethane film, a hybrid wavelength-selective responsive structure capable of reversible, programmable, and controllable motions is produced. By using the two-way light-driven shape memory composite, the bionic actuator is able to complete a series of tasks including accurate bending and mechanical gripping.

KEYWORDS: Prussian blue nanoparticles, reversible shape memory composite, jumping athlete, bionic actuators, programmable motions
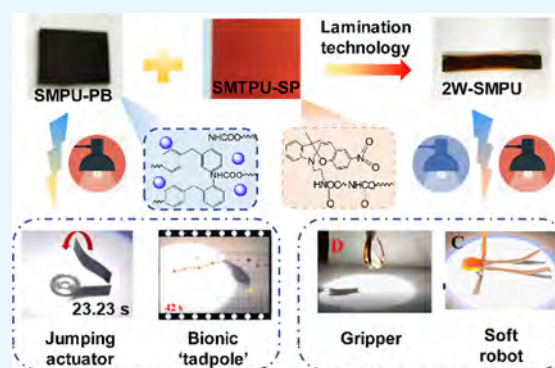
1. INTRODUCTION

For adapting to the complex and constant changing environment, natural organisms have evolved a variety of responsive behaviors, such as dynamical adjusting of body shape, color, and position, to enhance their survival ability.[1,2] In recent years, thanks to the inspiration of nature's biological behavior and the development of stimulus-responsive polymer materials, bionic intelligent actuators have made great progress in many aspects, for example, sensing environmental changes, feedback regulation, and performing tasks autonomously, which expanded the application scenarios.[3,4] One of the most interesting was the jumping motion, which played an important role in the survival of living organisms and allowed those slowly moving species to efficiently enable rapid hunting, escaping, overcoming large obstacles, and so forth.[5] Compared with the crawling actuator, jumping soft robots had the advantages of high efficiency and fast locomotion, which showed bright prospects in environment exploration and military applications.[6] Shape memory polymer (SMP) is one of the important materials for bionic intelligent actuators, which can fix a temporary shape under external force and return to the original shape upon various stimulations.[7] Nowadays, researchers have developed photo-,[8,9] electric-,[10,11] magnetic-,[12,13] and solvent-actuated SMPs.[14,15] Photo-response is a kind of remote non-contact control methods that can achieve fast, accurate, and remote actuation. More importantly, photo-actuated SMP can directly convert solar energy to mechanical

energy and improve the utilization efficiency of light energy. Thus, in recent years, photo-actuated SMPs have attracted widespread attention from researchers.[16,17] However, there are more research studies on one-way SMPs but less on two ways.[18−22] Two-way shape memory polymer (2W-SMP), named reversible SMP, can realize the temporary shape and the initial shape transformation only through the change of temperature or other stimulation.[23] 2W-SMPs have great applications in 4D printing,[24] artificial muscles,[25] surface microstructure control,[26] dynamic optical equipment,[27] flexible actuators, and sensors.[28,29]

Photo-actuated reversible SMPs are divided into two categories. One is liquid crystal elastomers (LCEs) containing azobenzene groups. These LCEs undergo deformation and shape recovery under different wavelengths of light irradiation.[30] The other is photo-thermal SMP composites. The photo-thermal effect nanoparticles are doped into the bidirectional SMP matrix and absorb a certain wavelength of light, such as ultraviolet (UV) light, visible light, or near-infrared
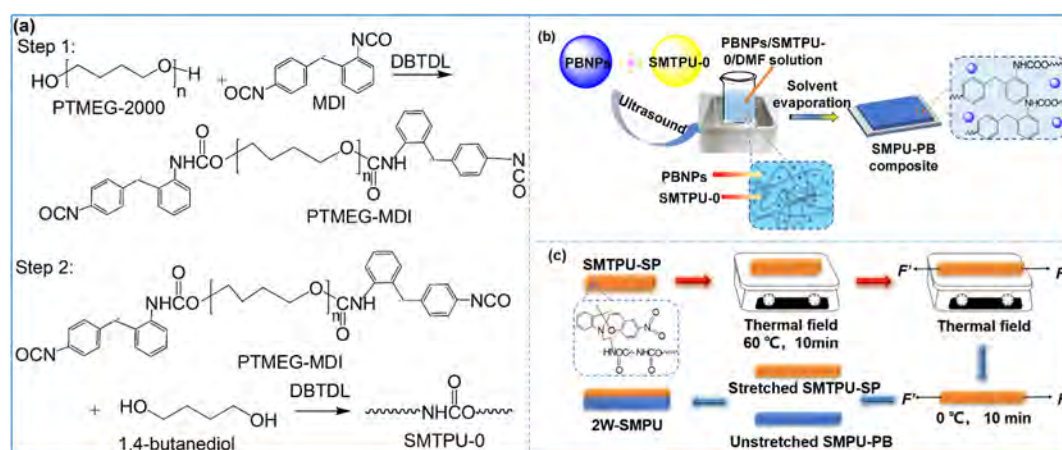
Figure 1. (a) Preparation process of SMTPU-0. (b) Preparation process of SMPU-PB. (c) Preparation process of 2W-SMPU.

(NIR) light, and convert light energy into thermal energy, which can promote the SMP matrix to achieve shape memory behavior.[31] It should be noted that these reversible photothermal shape memory matrices are thermally responsive SMPs, like semi-crystalline ethylene-vinyl acetate copolymer (EVA),[32] semi-crystalline polyurethane (PU),[33] semi-crystalline poly(ε-caprolactone) (PCL),[34] and so on. In 2018, Wang et al.[34] had designed and prepared a series of photo-actuated 2W-SMP composites by incorporating very small amounts of polydopamine (PDA) nanospheres into semi-crystalline PCL copolymers. PDA nanospheres owned good photothermal effect because of their strong absorption of light energy. When the light was switched on and off, the composites showed excellent two-way shape memory effects (2W-SMEs). Except for the pure two-way SMPs, the special double-layer structure can also be regarded as an ideal construction, which exhibits two-way shape memory effect.[35] However, the special double-layer structure has no application in the photo-actuated reversible SMPs.

Prussian blue nanoparticles (PBNPs) are a kind of the most classic Fe^{2+} and Fe^{3+} mixed valence hexacyanoferrate cubic nanoparticles, and the chemical formula is $Fe_4[Fe(CN)_6]_3$. For the PBNPs, $C\equiv N$ bond acts as a coordination bond bridge to connect Fe^{2+} and Fe^{3+}, Fe^{2+} is connected to C atom, and Fe^{3+} is connected to N atom.[36,37] Because of the excellent structure, PBNPs have outstanding photophysical, magnetic, electrochemical, and electrochromic properties.[38] As an excellent near-infrared photothermal agent, the PBNPs have strong absorption at 808 nm near-infrared (NIR) light, which is widely used in sensors, magnetic devices, energy storage, and batteries. In order to prepare nanoparticles with a controllable particle size and good dispersibility, citric acid is usually used as the surface protective agent. The citric acid-modified PBNPs can be prepared by mixing $FeCl_3$, citric acid and potassium ferricyanide $K_4[Fe(CN)_6]$ aqueous solution. The citric acid can coordinate with Fe^{3+} through its carboxyl group, and can effectively control the particle size of PBNPs during the reaction of Fe^{3+} and ferrocyanide to form Prussian blue crystals.[36]

The innovations of the study are as follows: first, the citric acid-modified PBNPs are doped into shape memory polymer matrix as photothermal conversion particles for the first time to prepare NIR-responsive shape memory polyurethane composite. The photothermal effect of Prussian blue nanoparticles is similar to that of gold nanoparticles,[39] but it is significantly

more cost effective than gold nanoparticles, which is a major advantage for the Prussian blue nanoparticles. Second, a bionic "athlete" prepared by SMPU-PB has photomechanical jumping behavior, and a bionic "tadpole" also had directed and controlled motion upon 808 nm NIR light irradiation. Most of the SMPs are used in the deformation expansion area; however, there are a few SMPs in jumping, swimming, and other dynamic actions. This experiment is the first to complete the photo-mechanical jumping and light-driven swimming motion of shape memory polyurethane composite. Third, a two-way SMP composite with UV light and NIR light response shape memory effect is produced, and it has the advantages of remote control, programmability, and high sensitivity, which will be applied to controllable soft robots, bio-robotic grasping hand with three fingers, bionic actuators, and other fields.

2. MATERIALS AND METHODS

2.1. Materials. Citric acid, anhydrous ferric chloride ($FeCl_3$), and potassium ferrocyanide $K_4[Fe(CN)_6]$ were all from Shanghai Aladdin Reagent Co., Ltd. N,N-dimethylformamide (DMF), analytically pure, was from Tianjin Fengchuan Chemical Reagent Technology Co., Ltd. Deionized water was from Harbin Institute of Technology. 365 nm UV-actuated shape memory polyurethane (SMTPU-SP) and thermal-actuated shape memory polyurethane (SMTPU-0) were both from our laboratory, and their preparation process and properties are seen in ref 40.

2.2. Preparation of Photo-Actuated Reversible SMP Composites. *2.2.1. Preparation of Citric Acid-Modified Prussian Blue Nanoparticles.* According to the reference,[36] the citric acid-modified PBNPs were prepared. A certain amount of $FeCl_3$ and $K_4[Fe(CN)_6]$ were added into 20 mL of deionized water containing 0.05 mmol citric acid, and the final concentrations of $FeCl_3$ and $K_4[Fe(CN)_6]$ were both 1.0 mmol L^{-1}. The above solutions were heated to 60 °C; the $K_4[Fe(CN)_6]$ solution was dropwise added into the $FeCl_3$ solution under stirring at 60 °C, and the color of the solution changed to blue; then the solution was stirred for 30 min and cooled to room temperature. After that, an equal volume of acetone was added into the blue solution, and it was placed at room temperature for 30 min. The solution was centrifuged at 10,000 rpm for 60 min to collect the nanoparticles, and the process was repeated three times. Finally, the collected PBNPs were dried at 50 °C for 12 h, and the citric acid-modified PBNPs were prepared successfully.

2.2.2. Preparation of NIR-Actuated Shape Memory Polyurethane Composite (SMPU-PB). First, 0.46 g of PBNPs was put into 10 mL of N,N-dimethylformamide (DMF) solvent and ultrasound for 6 h to make them evenly dispersed in DMF solvent. Then, 10 g of thermal-actuated shape memory polyurethane matrix (SMTPU-0, the preparation process is shown in Figure 1a and the Supporting
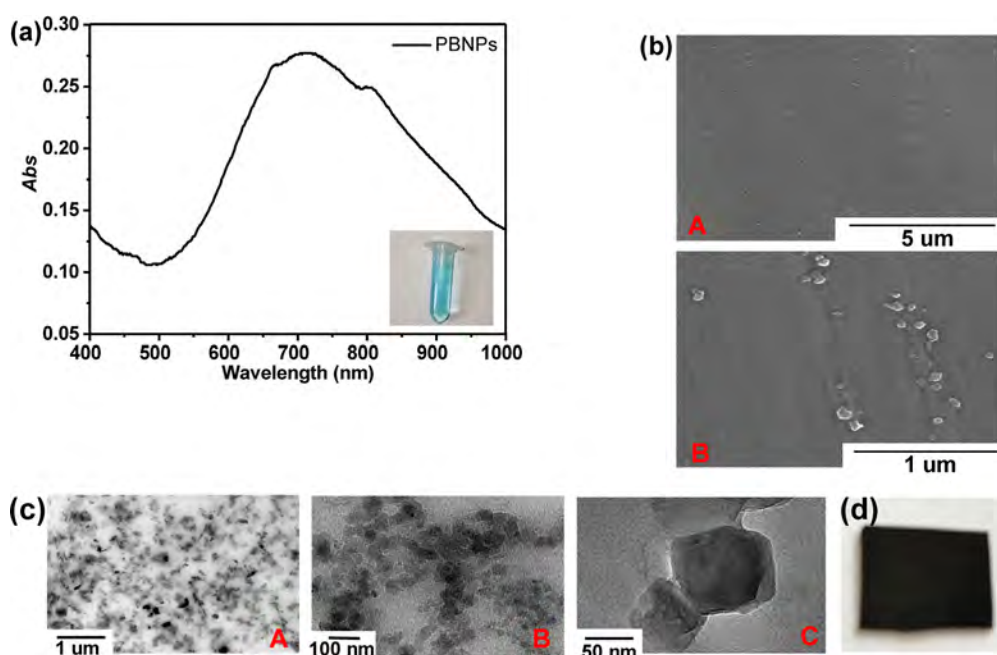
Figure 2. (a) PBNP aqueous suspension (50 ppm) and its UV−vis spectrum. (b) SEM images of PBNPs and their distribution in SMTPU-0 matrix. (c) TEM images of PBNPs and their distribution in SMTPU-0 matrix. (d) Photo of SMPU-PB.

Information) was dissolved in the DMF solvent, and PBNP solution was mixed well with the SMTPU-0 solution. After that, the mixture solution was poured into a Teflon mold and was held in a vacuum oven at 80 °C for 24 h; finally, citric acid-modified PBNP/polyurethane polymer thin film was prepared, named SMPU-PB. The preparation process is shown in Figure 1b.

2.2.3. Preparation of Photo-Actuated Reversible Shape Memory Polymer Composites (2W-SMPU). SMTPU-SP (43 mm*4 mm*1 mm) was put into 60 °C environment and stretched to a length of 47 mm; then, it was put into 0 °C environment for 10 min and the temporary shape was fixed without external force. Afterward, a little of glue was put on the surface of the non-stretched SMPU-PB (47 mm*4 mm*1 mm); then, it was bonded to the pre-stretched SMTPU-SP to get a reversible shape memory composite film, named 2W-SMPU (47 mm*4 mm*2 mm); among them, SMTPU-SP was stretched by about 9.3%. The preparation process is shown in Figure 1c.

2.3. Characterization. The molecular structure of SMTPU-0 was tested using an AVATAR360 spectrometer (FTIR) and ^{1}H NMR (The solvent was CDCl$_3$). The UV−vis absorption spectra of PBNPs were tested using a Daojin UV-3600 UV−visible spectrophotometer. The test range was 400−1000 nm. The morphological characteristics of PBNPs and the dispersion properties of PBNPs in the polyurethane matrix were observed using a JEM-1200 scanning electron microscope (SEM, JEOL Corporation of Japan) and 2100F transmission electron microscope (TEM, JEOL Corporation of Japan). The glass-transition temperature of SMPU-PB was tested using a Mettler Toledo DSC1 differential scanning calorimeter. The test conditions were a N$_2$ atmosphere, the flow rate of 10.00 mL min^{-1}, the temperature rise/fall rate of 5 °C min^{-1}, and the temperature range of 0−100 °C. Thermal weightlessness and the thermal stability of SMPU-PB were tested using a TGA/DSC1 synchronous thermal analyzer, produced by METTLER-TOLEDO Corporation, Switzerland. The test conditions were a temperature range of 25−600 °C, a heating rate of 10 °C min^{-1}, N$_2$ atmosphere, and a weight of 5−10 mg. The temperature−time properties of SMPU-PB and SMTPU-0 were analyzed under 808 nm NIR light irradiation (1.5 mW cm^{-2}, Beijing Newbit Technology Co., Ltd.), and at regular intervals, an infrared thermometer was used to test the surface temperature of the samples. The tensile properties of SMPU-PB and SMTPU-0 were tested using a microcomputer tensile testing machine SBA-10 (Chongqing Haco

Technology Co., Ltd.). The sample size was prepared according to GB/T528-2009. The tensile speed was 20 mm min^{-1}. The NIR-actuated shape memory performance test is as follows: first, the SMPU-PB sample was heated to 60 °C for 10 min; then, it was bent in half and cooled to 0 °C under external force for 10 min to fix the temporary shape. Finally, the sample was irradiated in 808 nm NIR light for 2 min to measure the deformation recovery. The schematic diagram is seen in the Supporting Information, Figure S1. The photo-actuated reversible shape memory performance test is as follows: first, the 2W-SMPU sample was put under 365 nm UV light irradiation to bend the sample until the bending angle no longer changes; the required time T_1 and bending angle θ_1 were recorded. Then, it was irradiated with 808 nm NIR light to recover the shape until the bending angle no longer changes; the required time T_2 and the bending angle θ_2 were recorded. Therefore, the time T for one cycle was ($T_1 + T_2$), and the changed angle θ was ($\theta_1 - \theta_2$). The schematic diagram is seen in the Supporting Information, Figure S2.

3. RESULTS AND DISCUSSION

3.1. Structural Analysis of SMPU-PB. Figure 2a shows an aqueous suspension of 50 ppm PBNPs and its UV−vis spectrum. It can be seen from Figure 2a that the aqueous suspension was blue uniformly, the dispersibility of PBNPs was very good, and there was no particle precipitation within 2 weeks. As a surface protectant, citric acid can coordinate with Fe^{3+} through its carboxyl group, effectively preventing nanoparticle aggregation and improving the dispersion and stability of nanoparticles in solution.[36] The UV−vis curve of PBNPs was in the range of 400−1000 nm. Because of electric charge-transfer transition between Fe^{2+} and Fe^{3+} of the PBNP structure, there was a wider absorption band between 600 and 900 nm. The maximum absorption peak was at 717 nm, which was the characteristic absorption peak of the PBNPs. Besides, there was a small absorption peak at 806 nm. Therefore, the modified PBNPs had a strong absorption capability in the NIR light region between 700 and 900 nm and were considered to be an excellent light-to-heat conversion agent.

The distribution of PBNPs in the shape memory polyurethane matrix was characterized by SEM and TEM. As shown
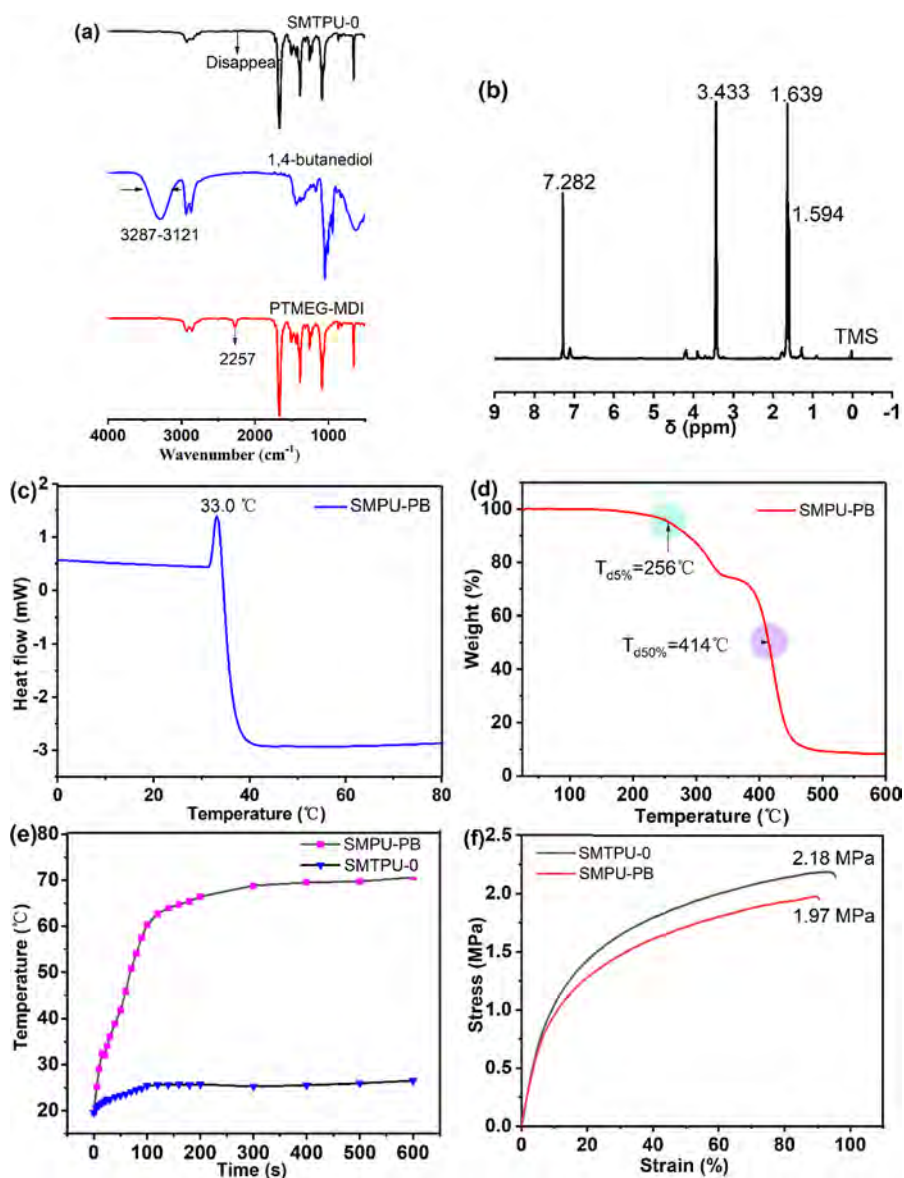
Figure 3. (a) FTIR spectra of PTMEG-MDI, 1,4-butanediol, and SMTPU-0. (b) ^{1}H NMR of SMTPU-0. (c) DSC curve of SMPU-PB. (d) TGA curve of SMPU-PB. (e) Temperature–time curve of SMPU-PB and SMTPU-0 upon 808 nm NIR light irradiation. (f) Stress–strain curves of SMPU-PB and SMTPU-0, respectively.

in Figure 2b-A,B, SEM images of SMPU-PB composite are magnified to 25,000 times and 100,000 times. In Figure 2b, the white particles are PBNPs, the black part is SMTPU-0 matrix resin, and the white particles (i.e., PBNPs) are evenly distributed in the matrix resin. This was because the PBNPs modified by citric acid had a relatively uniform particle size and high surface electric charge, which effectively prevented the particles' aggregation and improved the dispersion of nanoparticles in the matrix. Also, TEM was used to characterize the microscopic morphology of PBNPs and their distribution in SMTPU-0 matrix (Figure 2c). From the TEM images in Figure 2c-A,B, it can be visually observed that the PBNPs were uniformly distributed in the polyurethane matrix. Besides, it can be seen in Figure 2c-C that the PBNPs we prepared were cubic crystal structures with a size of about 50 nm. This was mainly due to the action of citric acid surface modifiers. The coordination interaction of the Fe^{3+} ion and the carboxyl groups of citric acid made the PBNPs more uniform in the

matrix. In Figure 2d, it can be seen that the surface of SMPU-PB was smooth and uniform in color and had no cracks, indicating that the citric acid-modified PBNPs had good interfacial bonding performance with the SMTPU-0 matrix resin. Additionally, there were no cracks at the junction of the nanoparticles and the matrix resin in Figure 2c-B. Therefore, the experiments show that the citric acid-modified PBNPs can be well compounded with the SMTPU-0 matrix resin.

The infrared spectrum of the SMTPU-0 matrix is shown in Figure 3a. On the PTMEG-MDI infrared spectra, 2257 cm^{-1} was the −NCO characteristic absorption peak. On the 1,4-butanediol infrared spectra, 3287−3121 cm^{-1} was the −OH characteristic absorption peak. Both the −NCO absorption peak in the PTMEG-MDI spectra and the hydroxyl group characteristic absorption peak in the 1,4-butanediol spectra disappeared in the SMTPU-0 spectra, indicating that PTMEG-MDI reacted with 1,4-butanediol and formed SMTPU-0. Figure 3b shows the ^{1}H NMR of SMTPU-0, where the
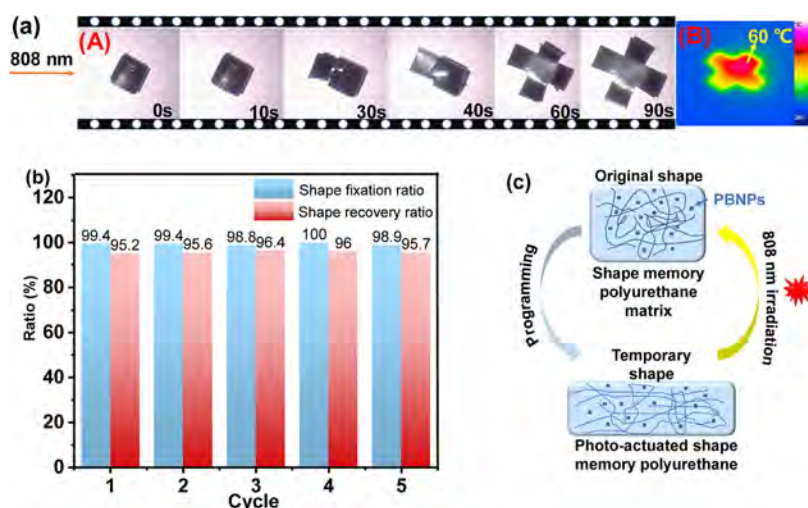
Figure 4. (a) Shape recovery process (A) and thermal infrared image (B) of the "box" upon 808 nm NIR light irradiation. (b) Shape fixation ratio and shape recovery ratio of SMPU-PB for five cycles. (c) Shape memory mechanism of NIR-actuated SMPU-PB.

chemical shift at δ = 7.282 ppm was the characteristic peak of hydrogen on the benzene ring, the chemical shift at δ = 3.433 ppm was the characteristic peak of CH_2 associating with the PTMEG and carbamate, and the chemical shift at δ = 1.594–1.639 ppm was the characteristic peak of $-CH_2$ associating with 1,4-butanediol and carbamate, therefore confirming the successful preparation of the SMTPU-0 polymer.

Differential scanning calorimetry (DSC) test can characterize the shape memory transition temperature of SMPU-PB. It can be seen from Figure 3c that the soft segment melting point of SMPU-PB was 33.0 °C, which was also the shape memory transition temperature (T_{trans}). Over the T_{trans}, the soft segment crystal region was melted and the molecular chains of the soft segments were easy to move, which can be shaped by external stress. If the deformed SMPU-PB was cooled to lower than the T_{trans}, the temporary shape can be fixed. During the shape memory process, SMPU-PB was heated to 60 °C for shaping and then cooled to 0 °C to fix the temporary shape through soft segment crystallization.

TGA was used to characterize the thermal stability of the shape memory composite. As shown in Figure 3d, the TGA curve of SMPU-PB was flat below 200 °C, indicating that the weight loss was very small, and there was hardly any decomposition in the polymer composite. In the range of 300−500 °C, the composite underwent rapid decomposition, and when the temperature reached 500 °C, the composite was almost completely decomposed. The 5% decomposition temperature ($T_{dec,5\%}$) and 50% decomposition temperature ($T_{dec,50\%}$) of SMPU-PB were 256 and 414 °C, respectively. In the temperature−time curve of SMPU-PB upon 808 nm NIR light irradiation (Figure 3e), the surface temperature of the composite was 70.6 °C after irradiation for 600 s; therefore, it did not have any thermal stability damage in the shape memory progress.

We also tested the temperature−time curves of SMPU-PB and pure shape memory polyurethane SMTPU-0 upon 808 nm NIR light irradiation (Figure 3e). With the increase of irradiation time, the surface temperature of SMPU-PB increased continuously, and it increased almost linearly from 0 to 100 s. After irradiation for 25 and 100 s, the surface temperature was 34.0 and 60.3 °C, respectively, and then it increased slowly. After irradiation for 600 s, the surface

temperature of SMPU-PB was 70.6 °C. The photothermal effect of PBNPs was similar to that of graphene oxide; specifically, the graphene oxide/SMPU photothermal composite can reach 67.6 °C under 808 nm NIR irradiation,[41] and the PU-GO film reached over 83 °C under NIR irradiation.[42] In the DSC test, the melting point of the soft segment of SMPU-PB was 33.0 °C, so the surface temperature can reach the T_{trans} upon 808 nm NIR light irradiation, driving the SMPU-PB to restore its original shape. In contrast, with the increase of irradiation time, the surface temperature of SMTPU-0 increased slowly, and after irradiation for 600 s, the surface temperature of SMTPU-0 increased to 26.5 °C, an increase of 6.9 °C, which was much lower than its glass-transition temperature (at 29.7 °C[40]). Therefore, pure shape memory polyurethane SMTPU-0 cannot recover to its original shape under NIR light irradiation.

The mechanical loading properties of SMTPU-0 and SMPU-PB were tested using a microcomputer tensile testing machine, and the stress−strain curves are shown in Figure 3f. The tensile strengths of SMTPU-0 and SMPU-PB were 2.18 and 1.97 MPa, respectively, which indicated that PBNPs reduced the tensile strength of the SMP matrix. The maximum elongation at break of SMTPU-0 and SMPU-PB was 93.75 and 89.56%, respectively. Because the doping of PBNPs into the polymer matrix could form stress concentration points, during the stretching process, these stress concentration points formed stress defects, which reduced the tensile strength and elongation at break.

3.2. Photo-Actuated Shape Memory Properties. At present, SMP is moving toward a higher degree of intelligence applications such as multi-stimuli actuations and bionic motions. To verify the shape memory functions, we first tested the shape memory process of a "box" fabricated by SMPU-PB, which is shown in Figure 4a. After irradiation with 808 nm NIR light for 90 s, the "box" shape unfolded and recovered to its original shape, proving that SMPU-PB had NIR light actuation shape memory capability (Figure 4a-A). The thermal infrared image showed that the "box" was evenly heated upon 808 nm NIR light irradiation, and after 90 s, the surface temperature was as high as 60 °C (Figure 4a-B). Figure 4b shows the results of shape memory properties of the SMPU-PB for five cycles. The shape fixation ratio in the five
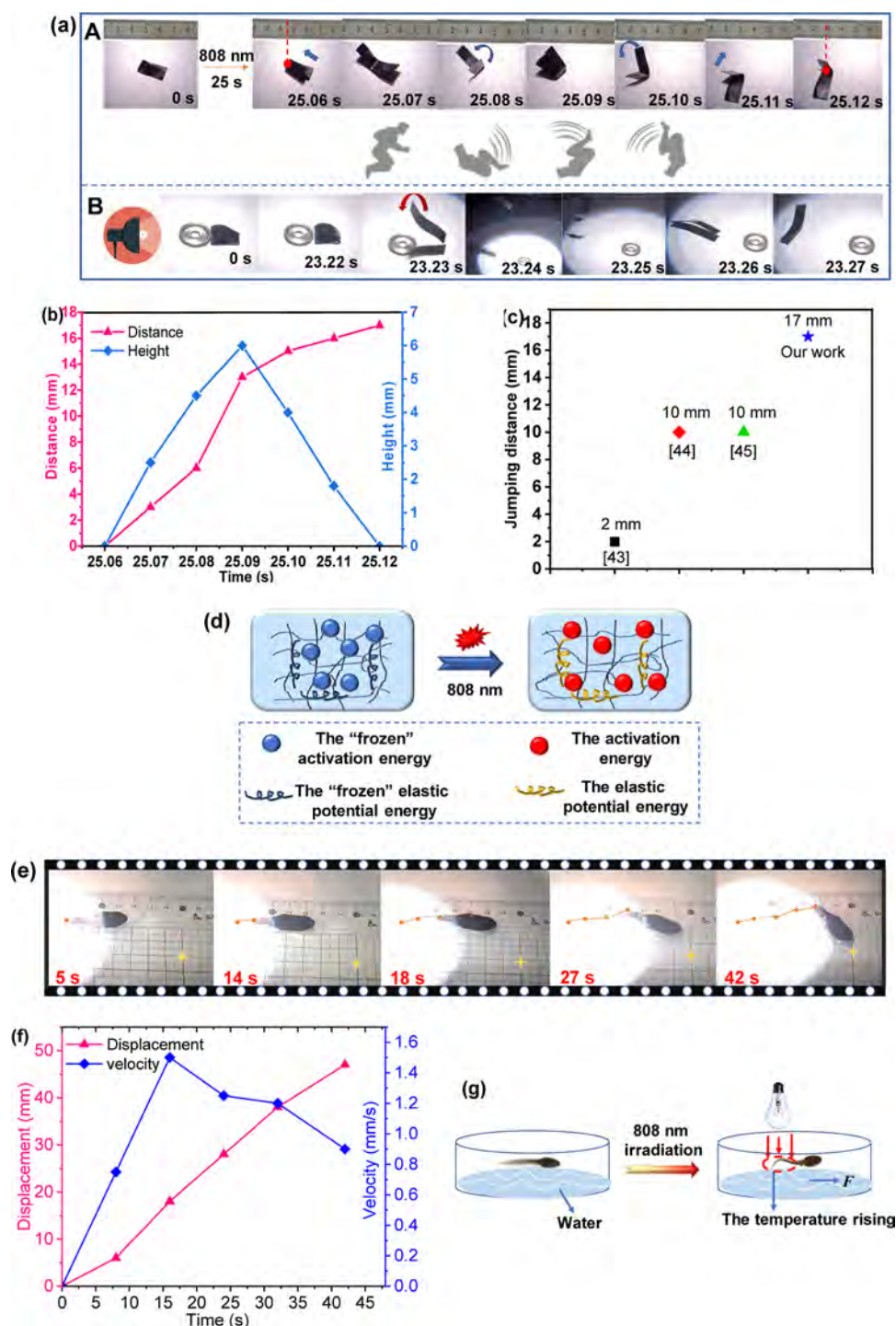
Figure 5. (a) "Jump" process (A) and "cross obstacle" process (B) of SMPU-PB under 808 nm NIR light irradiation. (b) Distance−time and height−time curves of the "jump" process. (c) Comparison of jumping distance with other literature studies. (d) Photomechanical jumping mechanism of the "athlete" produced by SMPU-PB. (e) Bionic "tadpole" made by SMPU-PB moved toward the yellow target upon 808 nm NIR light irradiation. (f) Displacement−time curve and velocity−time curve of the bionic "tadpole". (g) Swimming mechanism of the bionic "tadpole".

cycles was 99.4, 99.4, 98.8, 100, and 98.9%, respectively, and the shape recovery ratio in the five cycles was 95.2, 95.6, 96.4, 96.0, and 95.7%, respectively. The changes in the shape fixation ratio and shape recovery ratio were very small, almost unchanged, which proved that SMPU-PB cannot fail after repeated shape memory cycles. Also, the shape recovery ratio was not 100%. This may be because the SMPU-PB composite was a thermoplastic material, and during the shape fixation

process, the external force may cause permanent deformation of a small part of molecular chain which cannot be recovered during the shape recovery process.

Figure 4c is the NIR-actuated shape memory mechanism of SMPU-PB. For achieving shape memory properties, both a reversible phase and a stationary phase are required in the polymer molecular structure. The reversible phase is a phase state that can respond to external stimuli and determines the
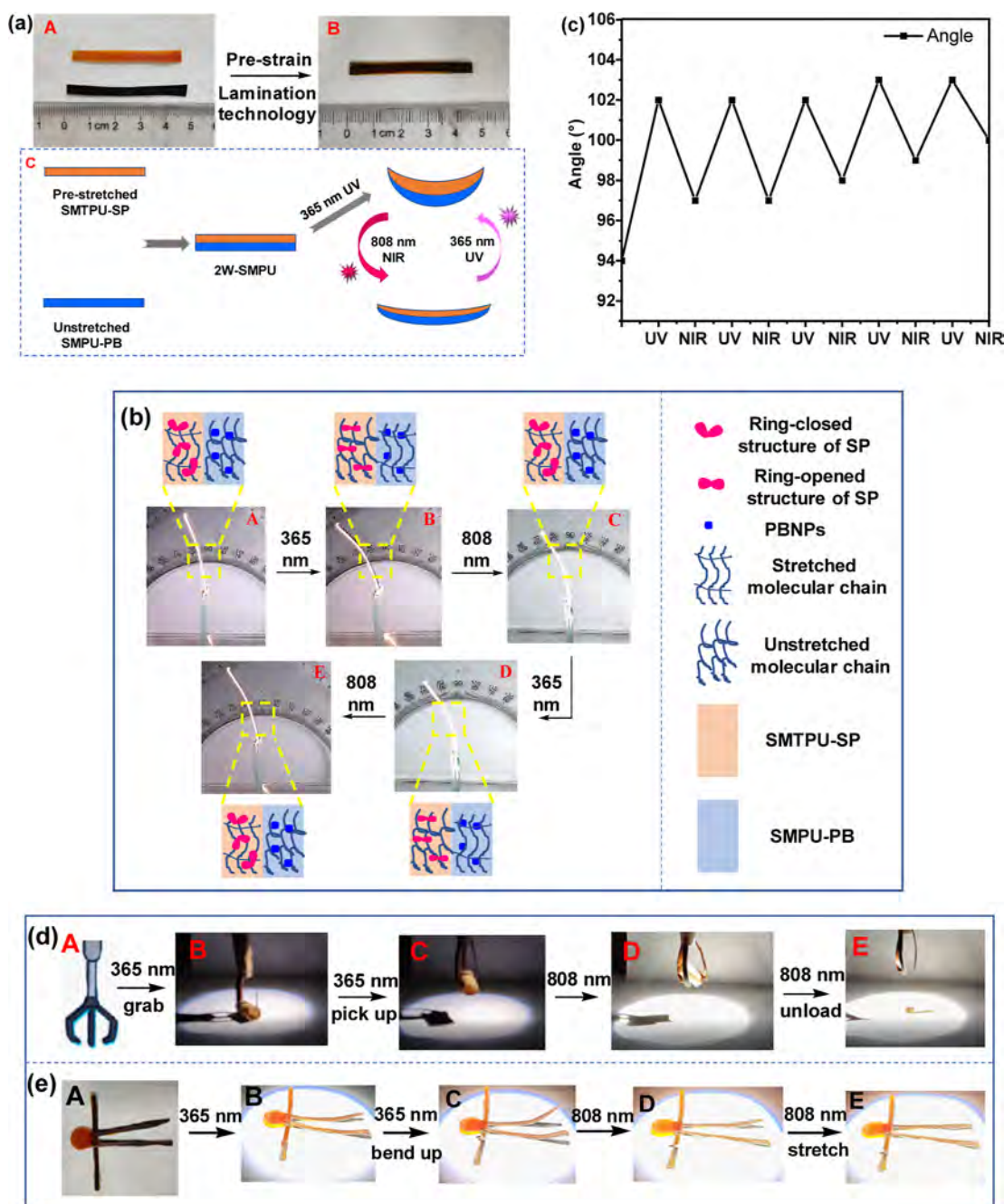
Figure 6. (a) Preparation of reversible shape memory thin film 2W-SMPU (A,B) and the shape morphing diagram of reversible photo-actuated 2W-SMPU (C). (b) Photos of UV−NIR-actuated reversible shape morphing process (SMTPU-SP pre-strain 9.3%, vertical placement, two cycles) and UV−NIR-actuated reversible shape morphing mechanism. (c) Angle changes of 2W-SMPU upon light irradiation of different wavelengths (SMTPU-SP pre-strain 9.3%, vertical placement, five cycles). (d) Mechanical gripper (A) and its gripping photos under different light irradiations (B-E). (e) Photos of a bionic athlete "stretching motion" processes.

shape fixing process of the SMP; the stationary phase can be a physical crosslinking point or a chemical crosslinking point, which determines the shape recovery process of the SMP. Thermoplastic shape memory polyurethane SMTPU-0 is a typical thermal-actuated SMP. Among them, the soft segment (PTMEG-2000) of the polymer is the reversible phase and the hard segment (MDI) is the stationary phase. Under thermal field stimulation, the soft-segment crystallization of SMTPU-0 is melted, and the SMP recovered from the temporary shape to the original shape. Doping PBNPs into shape memory polyurethane matrix can enable the SMP composites with

NIR light response. When the temperature is higher than the melting point temperature of the soft segments and lower than the melting point temperature of the hard segments of the SMTPU-0 matrix, SMPU-PB can be programmed to a new shape upon external force. When the temperature drops below the melting point temperature of the soft segments, the new shape or temporary shape can be fixed. At room temperature, SMPU-PB is irradiated with 808 nm NIR light, the PBNPs have an excellent NIR photothermal effect with Fe^{2+} and Fe^{3+}, and they can convert light energy into heat energy and transfer the energy to the polyurethane matrix. When the NIR light is

irradiated for 25 s, the surface temperature of SMPU-PB rises to 34 °C, which exceeds the melting point temperature of the soft segment; therefore, the polyurethane's soft segment melts and the temporary shape recovers to the original shape.

Also, we prepared an "athlete" (a size of 32 mm*8 mm*0.25 mm, a weight of 97.5 mg); Figure 5a-A shows the light-actuated jumping motion of the SMP composite-based "athlete", and it can begin to "jump" after 808 nm NIR light irradiation for 25.6 s and moved 17 mm in 0.06 s. Also, the simple "athlete" can jump over obstacles in Figure 5a-B, and after five times, the photomechanical "cross obstacle" performance did not decrease significantly. (The photomechanical "cross obstacle" performance is shown in the Supporting Information, Table S1.) In Figure 5b, it can be seen that the jumping distance was 17 mm, and the highest height was 6.5 mm. The jumping distance of the smart "athlete" was compared with that reported in other literature studies,[43−45] as shown in Figure 5c. The results showed that the jumping distance of the common "athlete" was generally below 10 mm; however, our work can reach over 15 mm. The photo-mechanical jumping mechanism of the "athlete" is as follows (Figure 5d): when the "athlete" is at high temperature, the soft segment molecular chain moves faster and has a higher activation energy. Then it cools down rapidly to fix the temporary shape, and, at the meantime, the activation energy is stored in the "frozen" soft segment molecular chain. Under the irradiation with NIR light, PBNPs absorb light energy and transform into heat energy, which is transferred to the shape memory polyurethane matrix to activate the "frozen" soft segment molecular chain, so the activation energy is released and converted into mechanical stress. The soft segment is a polyether glycol with good elasticity and has elastic potential energy; therefore, the "athlete" has photomechanical jumping behavior. The soft robots can move instantaneously like jumping athletes such as frogs and fleas and achieve fast jumps; therefore, they have broad application prospects in complex terrain, obstacles, and other environments. The photo-mechanical jumping of SMPU-PB by 808 nm irradiation is shown in the Supporting Information, Movie S1.

In addition, we produced a bionic "tadpole" which moved 47 mm toward the yellow target upon 808 nm NIR light irradiation for 42 s, of which the average velocity was 1.1 mm s^{-1} (Figure 5e). Also, the displacement−time curve and velocity−time curve of the bionic "tadpole" are shown in Figure 5f, and with the increase of irradiation time, the motion velocity increased first and then decreased. (The movement of the bionic "tadpole" is shown in the Supporting Information, Movie S2.) The motion velocity was faster than that of a "dolphin", but the mobility was lower than that of bionic "dolphin".[46] The swimming mechanism of the bionic "tadpole" is as follows (Figure 5g): because PBNPs have an excellent photothermal effect, under 808 nm NIR light irradiation, the surface temperature of SMPU-PB continues to rise, causing a temperature difference between the upper and lower surfaces, and the thermal expansion degrees of the upper and lower surfaces are different, and a surface tension gradient of water under the device appears between the irradiated and nonirradiated regions to propel the bionic "tadpole" device.[47] Therefore, under the action of surface tension, the bionic tadpole is driven to move forward and reaches the target. The bionic actuator driven by NIR light cannot be restricted by wires; the movement is more flexible, and the movement range is wider, which can expand the application area.

3.3. Two-Way Shape Memory Properties. Figure 6a−c shows the reversible two-way shape memory composite and its reversible shape memory behavior. In Figure 6a-A, SMTPU-SP thin film was stretched to 9.3% strain; then, the SMPU-PB film was laminated on the pre-stretched SMTPU-SP, and the UV−NIR-actuated reversible shape memory composite was prepared, named 2W-SMPU (Figure 6a-B). Figure 6a-C illustrates the reversible UV−NIR-actuated shape morphing diagram of 2W-SMPU. When irradiated with 365 nm UV light, the 2W-SMPU composite bends to the direction of SMTPU-SP, while under 808 nm NIR light irradiation, the 2W-SMPU composite has shape recovery and returns to its original shape. The reversible shape morphing mechanism is shown in Figure 6b. SMTPU-SP was prepared by grafting spiropyran molecule (SP), which had shape changes upon 365 nm UV light irradiation, and the shape change mechanism is shown in the Supporting Information, Figure S3. The C−O bond in the spiropyran molecule can be converted from a ring-closed structure to a ring-opened structure under UV light irradiation, and the C−O bond can be converted from a ring-opened structure to a ring-closed structure under a heating field or visible light irradiation.[48] The pre-stretched SMTPU-SP is in a temporary shape status, and the stress is frozen in it. When SMTPU-SP is irradiated with 365 nm UV light, the C−O bond of the spiropyran molecule is broken, resulting in isomerization to form ring-opened structures and rearrangement of the molecular structures and electron configuration. These ring-opened structures weaken the interaction force of the SMTPU-SP molecular chains; thus, the molecular chains of the soft segments become soft and move faster, facilitating the restoration of SMTPU-SP from a temporary shape to its original shape.[40] Therefore, SMTPU-SP shrinks and restores its original shape; at the same time, the molecular chains of SMPU-PB are stretched and the stretched stress is stored in it (Figure 6b-B). Macroscopically, the composite bends to the direction of SMTPU-SP, and the bending angle increases with the increase of irradiation time. When irradiated with 808 nm NIR light, the PBNPs have an excellent NIR photothermal effect, and they can convert light energy into heat energy and transfer the energy to the SMPU-PB matrix. With the increase of irradiation time, the heat energy of SMPU-PB is transferred to SMTPU-SP so that the spiropyran molecule of SMTPU-SP changes from the ring-opened structure to the ring-closed structure (Figure 6b-C). Macroscopically, SMPU-PB shrinks and recovers its original shape; at the same time, SMTPU-SP is stretched, which achieves a bidirectional shape morphing process. Under 365 nm UV irradiation, the recovery force of the pre-stretched SMTPU-SP causes the composite film to bend, until the recovery force is equal to the stretched stress of the underlying layer that it can reach a balanced status. While under 808 nm NIR light irradiation, the stretched SMPU-PB provides the recovery force to cause the composite film to return its original shape.[49] The most notable feature of this process is that it can directly express different shape changes without fabrication of the temporary shape in advance and this kind of design can work in a simple way to produce the shape memory composite.

We tested UV−NIR-actuated reversible shape morphing process, which is shown in the Supporting Information, Figure S4 (SMTPU-SP pre-strain 9.3%, horizontal placement). In order to eliminate the influence of gravity, we tested the vertical 90° shape morphing process of the sample (Figure 6b). With the continuous change of the irradiation wavelength, the

angle of the 2W-SMPU also changed. For the first cycle, under 365 nm UV light irradiation for 120 s, the sample bent from 94 to 102°, and the bending angle changed by 8°. Under 808 nm NIR light irradiation for 300 s, the sample changed from 102 to 97°, and the bending angle changed by 5°. In Figure 6c, we tested the angle changes of the 2W-SMPU after five cycles upon UV light and NIR light irradiation, respectively, which illustrated that 2W-SMPU could achieve reversible morphing upon different light irradiations. However, we should also see that the degree of bending of the 2W-SMPU composite decreased after many cycles, and the shape memory performance decreased.

Photo-actuated reversible shape memory polymer composites have programmable and controllable motions properties and have great potential for bionic intelligent actuators and soft robot applications. 2W-SMPU was used to prepare a three-arm-mechanical gripper capable of grabbing items (Figure 6d). After 15 s UV light irradiation, the three arms of the mechanical gripper were bent to grab the cylinder (a weight of 2 g) and move it upward (Figure 6d-B,C). After 26 s NIR irradiation, the bending angle of each arm of the mechanical gripper was reduced, and the cylinder was unloaded (Figure 6d-D,E). The deformation and recovery of the mechanical gripper were controlled by different light irradiations. After the mechanical gripper was irradiated with 365 nm UV light, the SMTPU-SP on the inner side of each arm recovered to the original shape, causing the mechanical arms to bend inward to complete the grasping action. Then, the mechanical gripper was irradiated with 808 nm NIR light, and the SMPU-PB on the outer side of each arm recovered to the original shape, resulting in the gripper's bending angle reduction and the unloading action completion. Also, the reversible shape memory composite was used to prepare a bionic "athlete". Figure 6eB−E shows the photos of "stretching motion" processes of a 2W-SMPU-based soft robot. When irradiated with 365 nm UV light, both "arms" and "legs" can bend up; after 70 s UV light irradiation, it achieved a maximum bending angle of 8°. Then, the soft robot moved down under 808 nm NIR light irradiation, and both "arms" and "legs" can move downward. The video of directional movement process is in the Supporting Information, named Movie S3.

4. CONCLUSIONS

An NIR photo-responsive shape memory polyurethane composite (SMPU-PB) is prepared by doping PBNPs into SMTPU-0. UV−vis test shows that the PBNPs have a strong absorption in the range of 700−900 nm NIR light, certificating that it is an outstanding photothermal absorber. SEM and TEM tests show that the citric acid-modified PBNPs have a particle size of about 50 nm and can be well dispersed in the shape memory polyurethane matrix. The NIR-actuated shape memory performance test shows the shape fixation ratio of 98.9% and the shape recovery ratio of 95.7% after repeating for five cycles. Besides, a reversible shape memory polymer composite 2W-SMPU with UV light and NIR light response shape memory effect is prepared by using lamination technology. 2W-SMPU had angle changes as the different light irradiations changed. The potential applications of 2W-SMPU in remote light-controlled soft robot motion, mechanical grippers, and bionic actuators are proved.

■ ASSOCIATED CONTENT

ⓈI Supporting Information

The Supporting Information is available free of charge at https://pubs.acs.org/doi/10.1021/acsapm.2c01911.

> Preparation of shape memory polyurethane matrix; schematic diagram of NIR-actuated shape memory performance test of SMPU-PB; deformation angle measurement method of photo-actuated reversible 2W-SMPU; UV-actuated shape change mechanism of SMTPU-SP; photos of UV-NIR-actuated reversible shape changes process; a brief introduction of the supplementary videos; and statistics of photomechanical "cross obstacle" performance of the sample actuator (PDF)

> Photomechanical jumping of SMPU-PB by 808 nm irradiation (MP4)

> Movement of the bionic "tadpole" (MP4)

> Directional movement process irradiated by 365 nm UV light and 808 nm NIR light (MP4)

> (MP4)

■ AUTHOR INFORMATION

Corresponding Author

Jinsong Leng − *Center for Composite Materials and Structures, Harbin Institute of Technology, Harbin 150080, P. R. China;* ⓞ orcid.org/0000-0001-5098-9871; Email: lengjs@hit.edu.cn

Authors

Xiaofei Wang − *Center for Composite Materials and Structures, Harbin Institute of Technology, Harbin 150080, P. R. China*

Yang He − *Center for Composite Materials and Structures, Harbin Institute of Technology, Harbin 150080, P. R. China*

Complete contact information is available at: https://pubs.acs.org/10.1021/acsapm.2c01911

Author Contributions

The manuscript was written through the contributions of all authors. All authors have given approval to the final version of the manuscript.

Notes

The authors declare no competing financial interest.

■ REFERENCES

(1) Jiang, X. F.; Tian, B. K.; Xuan, X. Y.; Zhou, W. Q.; Zhou, J. X.; Chen, Y. Q.; Lu, Y.; Zhang, Z. H. Cellulose membranes as moisture-driven actuators with predetermined deformations and high load uptake. *Int. J. Smart Nano Mater.* **2021**, *12*, 146−156.

(2) Du, L.; Xu, Z. Y.; Huang, C. L.; Zhao, F. Y.; Fan, C. J.; Dai, J.; Yang, K. K.; Wang, Y. Z. From a body temperature-triggered reversible shape-memory material to high-sensitive bionic soft actuators. *Appl. Mater. Today* **2020**, *18*, 100463.

(3) Pu, W.; Wei, F. A.; Yao, L. G.; Xie, S. X. A review of humidity-driven actuator: toward high response speed and practical applications. *J. Mater. Sci.* **2022**, *57*, 12202−12235.

(4) Chen, Y.; Zhao, X.; Li, Y.; Jin, Z. Y.; Yang, Y.; Yang, M. B.; Yin, B. Light- and magnetic-responsive synergy-controlled reconfiguration

of polymer nanocomposites with shape memory assisted self-healing performance for soft robotics. *J. Mater. Chem. C* **2021**, *9*, 5515−5527.

(5) Wang, J.; Zhao, T. H.; Fan, Y. Y.; Wu, H. M.; Lv, J. A. Leveraging bioinspired structural constraints for tunable and programmable snapping dynamics in high-speed soft actuators. *Adv. Funct. Mater.* **2022**, *33*, 2209798.

(6) Xu, L. L.; Xue, F. H.; Zheng, H. W.; Ji, Q. X.; Qiu, C. W.; Chen, Z.; Zhao, X.; Li, P. Y.; Hu, Y.; Peng, Q. Y.; He, X. D. An insect larvae inspired MXene-based jumping actuator with controllable motion powered by light. *Nano Energy* **2022**, *103*, 107848.

(7) Melly, S. K.; Liu, L. W.; Liu, Y. J.; Leng, J. S. Active composites based on shape memory polymers: overview, fabrication methods, applications, and future prospects. *J. Mater. Sci.* **2020**, *55*, 10975−11051.

(8) Xu, Z.; Ding, C.; Wei, D. W.; Bao, R. Y.; Ke, K.; Liu, Z. Y.; Yang, M. B.; Yang, W. Electro and light active actuators based on reversible shape-memory polymer composites with segregated conductive networks. *ACS Appl. Mater. Interfaces* **2019**, *11*, 30332−30340.

(9) Biswas, A.; Singh, A. P.; Rana, D.; Aswal, V. K.; Maiti, P. Biodegradable toughened nanohybrid shape memory polymer for smart biomedical applications. *Nanoscale* **2018**, *10*, 9917−9934.

(10) Gao, H.; Li, J. R.; Liu, Y. J.; Leng, J. S. Shape memory polymer solar cells with active deformation. *Adv. Compos. Hybrid Mater.* **2021**, *4*, 957−965.

(11) Gong, X. B.; Liu, L. W.; Liu, Y. J.; Leng, J. S. An electrical-heating and self-sensing shape memory polymer composite incorporated with carbon fiber felt. *Smart Mater. Struct.* **2016**, *25*, 035036.

(12) Zhao, F.; Rong, W. B.; Wang, L. F.; Sun, L. N. Magnetic actuated shape-memory helical microswimmers with programmable recovery behaviors. *J. Bionic Eng.* **2021**, *18*, 799−811.

(13) Yang, L. P.; Zhang, G. G.; Zheng, N.; Zhao, Q.; Xie, T. A metallosupramolecular shape-memory polymer with gradient thermal plasticity. *Angew. Chem. Int. Ed.* **2017**, *56*, 12599−12602.

(14) Xue, J. Y.; Ge, Y. H.; Liu, Z. T.; Liu, Z. W.; Jiang, J. Q.; Li, G. Photo-programmable moisture-responsive actuation of a shape memory polymer film. *ACS Appl. Mater. Interfaces* **2022**, *14*, 10836−10843.

(15) Tian, T.; Wang, J.; Wu, S. S.; Shao, Z. J.; Xiang, T.; Zhou, S. B. A body temperature and water-induced shape memory hydrogel with excellent mechanical properties. *Polym. Chem.* **2019**, *10*, 3488−3496.

(16) Luo, W.; Liu, J. X.; Fang, C. H.; Liu, B. P.; Xia, H. T.; Li, H. J.; Huang, J. Templating assembly of NIR light-actuated TPU/SCNT-C-60 flexible structures with high conductivity and controllable recovery behavior. *Surf. Interfaces* **2021**, *25*, 101230.

(17) Pang, X. L.; Lv, J. A.; Zhu, C. Y.; Qin, L.; Yu, Y. L. Photodeformable azobenzene-containing liquid crystal polymers and soft actuators. *Adv. Mater.* **2019**, *31*, 1904224.

(18) Zhou, B.; Zheng, X. Y.; Kang, Z. T.; Xue, S. F. Modeling size-dependent thermo-mechanical behaviors of shape memory polymer Bernoulli-euler microbeam. *Appl. Math. Mech.* **2019**, *40*, 1531−1546.

(19) Adiyan, U.; Larsen, T.; Zárate, J. J.; Villanueva, L. G.; Shea, H. Shape memory polymer resonators as highly sensitive uncooled infrared detectors. *Nat. Commun.* **2019**, *10*, 4518.

(20) Liu, Z. C.; Zuo, B.; Lu, H. F.; Wang, M.; Huang, S.; Chen, X. M.; Lin, B. P.; Yang, H. A copper(i)-catalyzed azide-alkyne click chemistry approach towards multifunctional two-way shape-memory actuators. *Polym. Chem.* **2020**, *11*, 3747−3755.

(21) Fan, L. F.; Rong, M. Z.; Zhang, M. Q.; Chen, X. D. A very simple strategy for preparing external stress-free two-way shape memory polymers by making use of hydrogen bonds. *Macromol. Rapid Commun.* **2018**, *39*, 1700714.

(22) Xie, X.; Xu, X.; Zhu, Q. X.; Lu, S. R.; Li, Y. Q.; Bai, Y. K. Thermo- and near infrared light-induced reversible multi-shape memory materials for actuators and sensors. *Mater. Chem. Front.* **2022**, *6*, 1973−1981.

(23) Liu, Y. Y.; Wu, W.; Wei, J.; Yu, Y. L. Visible light responsive liquid crystal polymers containing reactive moieties with good processability. *ACS Appl. Mater. Interfaces* **2017**, *9*, 782−789.

(24) Li, A.; Challapalli, A.; Li, G. Q. 4D Printing of recyclable lightweight architectures using high recovery stress shape memory polymer. *Sci. Rep.* **2019**, *9*, 7621.

(25) Feng, F.; Plucinsky, P.; James, R. D. Phase transformations and compatibility in helical structures. *J. Mech. Phys. Solid.* **2019**, *131*, 74−95.

(26) Ellson, G.; Prima, M.; Ware, T.; Tang, X. L.; Voit, W. Tunable thiol-epoxy shape memory polymer foams. *Smart Mater. Struct.* **2015**, *24*, 055001.

(27) Zhou, L. L.; Hu, Q. Z.; Kang, Q.; Yu, L. Construction of liquid crystal droplet-based sensing platform for sensitive detection of organophosphate pesticide. *Talanta* **2018**, *190*, 375−381.

(28) Gao, H.; Li, J. R.; Zhang, F. H.; Liu, Y. J.; Leng, J. S. The research status and challenges of shape memory polymer-based flexible electronics. *Mater. Horiz.* **2019**, *6*, 931−944.

(29) Sun, L.; Wang, T. X.; Chen, H. M.; Salvekar, A. V.; Naveen, B. S.; Xu, Q. W.; Weng, Y. W.; Guo, X. L.; Chen, Y. H.; Huang, W. M. A brief review of the shape memory phenomena in polymers and their typical sensor applications. *Polymers* **2019**, *11*, 1049.

(30) Saed, M. O.; Gablier, A.; Terentjev, E. M. Exchangeable liquid crystalline elastomers and their applications. *Chem. Rev.* **2022**, *122*, 4927−4945.

(31) Luo, Q.; Chen, J.; Gnanasekar, P.; Ma, X. Z.; Qin, D. D.; Na, H. N.; Zhu, J.; Yan, N. A facile preparation strategy of polycaprolactone (PCL)-based biodegradable polyurethane elastomer with a highly efficient shape memory effect. *New J. Chem.* **2020**, *44*, 658−662.

(32) Su, X. J.; Li, H. Q.; Lai, X. J.; Chen, Z. H.; Zeng, X. R. 3D porous superhydrophobic CNT/EVA composites for recoverable shape reconfiguration and underwater vibration detection. *Adv. Funct. Mater.* **2019**, *29*, 1900554.

(33) Guan, X. Y.; Chen, H. R.; Xia, H.; Fu, Y. Q.; Yao, J. M.; Ni, Q. Q. Flexible energy harvester based on aligned PZT/SMPU nanofibers and shape memory effect for curved sensors. *Composites, Part B* **2020**, *197*, 108169.

(34) Wang, K. J.; Zhu, X. X. Two-way reversible shape memory polymers containing polydopamine nanospheres: light actuation, robotic locomotion and artificial muscles. *ACS Biomater. Sci. Eng.* **2018**, *4*, 3099−3106.

(35) Chen, S. J.; Hu, J. L.; Zhuo, H. T.; Zhu, Y. Two-way shape memory effect in polymer laminates. *Mater. Lett.* **2008**, *62*, 4088−4090.

(36) Shokouhimehr, M.; Soehnlen, E. S.; Hao, J. H.; Griswold, M.; Flask, C.; Fan, X. D.; Basilion, J. P.; Basu, S.; Huang, S. P. D. Dual purpose Prussian blue nanoparticles for cellular imaging and drug delivery: a new generation of T-1-weighted MRI contrast and small molecule delivery agents. *J. Mater. Chem.* **2010**, *20*, 5251−5259.

(37) Shokouhimehr, M.; Soehnlen, E. S.; Khitrin, A.; Basu, S.; Huang, S. P. D. Biocompatible Prussian blue nanoparticles: preparation, stability, cytotoxicity, and potential use as an MRI contrast agent. *Inorg. Chem. Commun.* **2010**, *13*, 58−61.

(38) Zhai, J. F.; Zhai, Y. M.; Wen, D.; Dong, S. J. Prussian blue/multiwalled carbon nanotube hybrids: synthesis, assembly and electrochemical behavior. *Electroanal* **2009**, *21*, 2207−2212.

(39) Karyakin, A. A. Prussian blue and its analogues: electrochemistry and analytical applications. *Electroanal* **2001**, *13*, 813−819.

(40) Wang, X. F.; He, Y.; Leng, J. S. Smart shape memory polyurethane with photochromism and mechanochromism properties. *Macromol. Mater. Eng.* **2022**, *307*, 2100778.

(41) Zhang, P.; Cai, F.; Wang, G. J.; Yu, H. F. UV-Vis-NIR light-deformable shape-memory polyurethane doped with liquid-crystal mixture and GO towards biomimetic applications. *Chin. J. Polym. Sci.* **2022**, *40*, 166−174.

(42) Zhou, L. M.; Liu, Q.; Lv, X. D.; Gao, L. J.; Fang, S. M.; Yu, H. F. Photoinduced triple shape memory polyurethane enabled by doping with azobenzene and GO. *J. Mater. Chem. C* **2016**, *4*, 9993−9997.

(43) Li, Y.; Li, J.; Liu, L.; Yan, Y.; Zhang, Q.; Zhang, N.; He, L.; Liu, Y.; Zhang, X.; Tian, D.; Leng, J.; Jiang, L. Switchable wettability and

adhesion of micro/nanostructured elastomer surface via electric field for dynamic liquid droplet manipulation. *Adv. Sci.* **2020**, *7*, 2000772.

(44) Hu, Y.; Liu, J. Q.; Chang, L. F.; Yang, L. L.; Xu, A. F.; Qi, K.; Lu, P.; Wu, G.; Chen, W.; Wu, Y. C. Electrically and sunlight-driven actuator with versatile biomimetic motions based on rolled carbon nanotube bilayer composite. *Adv. Funct. Mater.* **2017**, *27*, 1704388.

(45) Jeon, J.; Choi, J. C.; Lee, H.; Cho, W.; Lee, K.; Kim, J. G.; Lee, J. W.; Joo, K. I.; Cho, M.; Kim, H. R.; Wie, J. J. Continuous and programmable photomechanical jumping of polymer monoliths. *Mater. Today* **2021**, *49*, 97−106.

(46) Ma, S. D.; Li, X.; Huang, S.; Hu, J.; Yu, H. F. A light-activated polymer composite enables on-demand photocontrolled motion: transportation at the liquid/air interface. *Angew. Chem., Int. Ed.* **2019**, *58*, 2655−2659.

(47) Xuan, H. X.; Guan, Q. B.; Zhang, L. Z.; You, Z. W. Thermoplastic photoheating polymer enables 3D-printed self-healing light-propelled smart devices. *Adv. Funct. Mater.* **2021**, *31*, 2009568.

(48) Zhang, X. Z.; Zhou, Q. Q.; Liu, H. R.; Liu, H. W. UV light induced plasticization and light activated shape memory of spiropyran doped ethylene-vinyl acetate copolymers. *Soft Matter* **2014**, *10*, 3748−3754.

(49) Chen, S. J.; Hu, J. L.; Zhuo, H. T. Properties and mechanism of two-way shape memory polyurethane composites. *Compos. Sci. Technol.* **2010**, *70*, 1437−1443.